Università degli Studi di Padova
Facoltà di Ingegneria

Corso di Laurea Triennale
in Ingegneria delle Telecomunicazioni

VECTOR PERTURBATION TECHNIQUE

Candidato:
Alessandro Vianello
563030

Relatore:
Prof. Nevio Benvenuto

A.A. 2009/10

CONTENTS

ACRONYMS

AWGN	additive white Gaussian noise
CDMA	code division multiple access
DIV-MIMO	diversity systems multiple input multiple output
DSL	digital subscriber line
DOF	degree of freedom
ISI	intersymbol interference
LR	lattice reduction
MIMO	multiple input multiple output
MSE	mean square error
PHY	physical layer
QAM	quadrature amplitude modulation
QPSK	quaternary phase shift keying
SA-MIMO	smart antenna multiple input multiple output
SEP	symbol-error probability
SINR	signal to interference plus noise ratio
SM-MIMO	spatial multiplexing multiple input multiple output
SNR	signal to noise ratio
STC-MIMO	space-time coding multiple input multiple output
TDD	time division duplex
TH	Tomlinson–Harashima precoding
WLAN	wireless local area network
ZF	zero-forcing

INTRODUCTION

Theoretical results describing the sum capacity when using multiple antennas to communicate with multiple users in a known rich scattering environment have not yet been followed with practical transmission schemes that achieve this capacity. The vector perturbation technique introduced a simple encoding algorithm that achieves near-capacity at sum rates of tens of bits/channel use. The algorithm is a variation on channel inversion that regularizes the inverse and uses a "sphere encoder" to perturb the data to reduce the power of the transmitted signal. The technique is comprised of two parts: it has shown in the first part that while the sum capacity grows linearly with the minimum of the number of antennas and users, the sum rate of channel inversion does not. This poor performance is due to the large spread in the singular values of the channel matrix. It introduces regularization to improve the condition of the inverse and maximize the signal to interference plus noise ratio (SINR)[1] at the receivers. Regularization enables linear growth and works especially well at low signal to noise ratios (SNRs), but an additional step is needed to achieve near-capacity performance at all SNRs. In fact, looking in the second part, before the regularization of the channel inverse, a certain perturbation of the data using a "sphere encoder" can be chosen to further reduce the energy of the transmitted signal. The performance difference with and without this perturbation is shown to be dramatic. With the perturbation, we can achieve excellent performance at all SNRs.

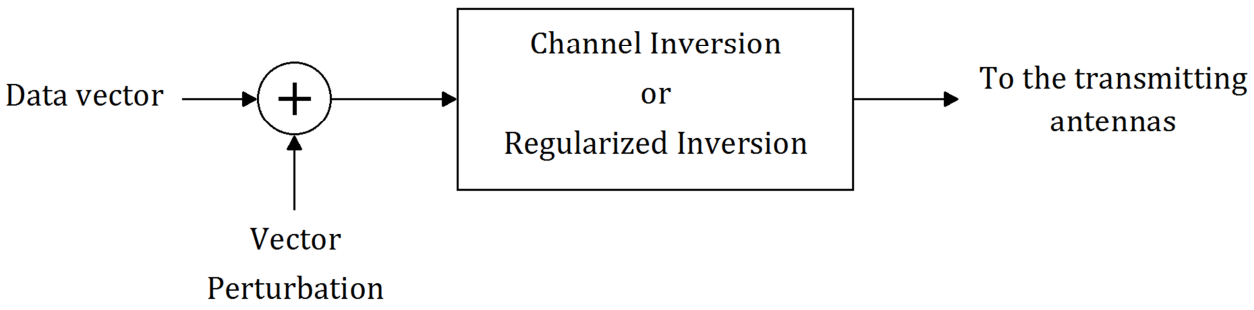

Figure 0.1 Block diagram representation of a generically "Vector Perturbation" system.

[1] The SINR also known as the carrier-to-interference ratio, is the quotient between the average received modulated carrier power and the average received co-channel interference power, i.e. cross-talk, from other transmitters than the useful signal.

Chapter 1

MIMO SYSTEMS [9]

Multi-antenna based multi-input multi-output (MIMO) communications first burst onto the scene in the mid-1990s. The pioneering work by Telatar, Foschini and Gans at Bell Labs demonstrated that MIMO in a wireless communication system can greatly improve performance, as much as one order of magnitude or more, without requiring any additional bandwidth. In the decade since, thousands of research papers have been written on the topic dealing with both physical layer (PHY) and network layer ramifications of the technology. MIMO has gone through the adoption curve for commercial wireless systems to the point that today, all high throughput commercial standards (i.e., WiMAX, Wi-Fi, cellular, etc.) have adopted MIMO as part of the optional, if not mandatory, portions of their standards.

1.1 Introduction to MIMO

A MIMO wireless system consists of *M*-transmit antennas and *K*-receive antennas; the spectral efficiency can (for large signal-to-noise ratios) in principle grow linearly with the minimum over the number of transmit and receive antennas. However, unlike phased array systems where a single information stream is transmitted on all transmitters and then received at the receiver antennas, MIMO systems transmit different information streams, say x_1, x_2 and x_3, on each transmit antenna. These are independent information streams being sent simultaneously and in the same frequency band. At first glance, one might say that the transmitted signals interfere with one another. In reality, however, the signal arriving at each receiver antenna will be a linear combination of the *M* transmitted signals. Figure 1.1 shows a MIMO system with three transmit and three receive antennas. The received signals y_1, y_2, y_3 at each of the three received antennas are a linear combination of x_1, x_2 and x_3.

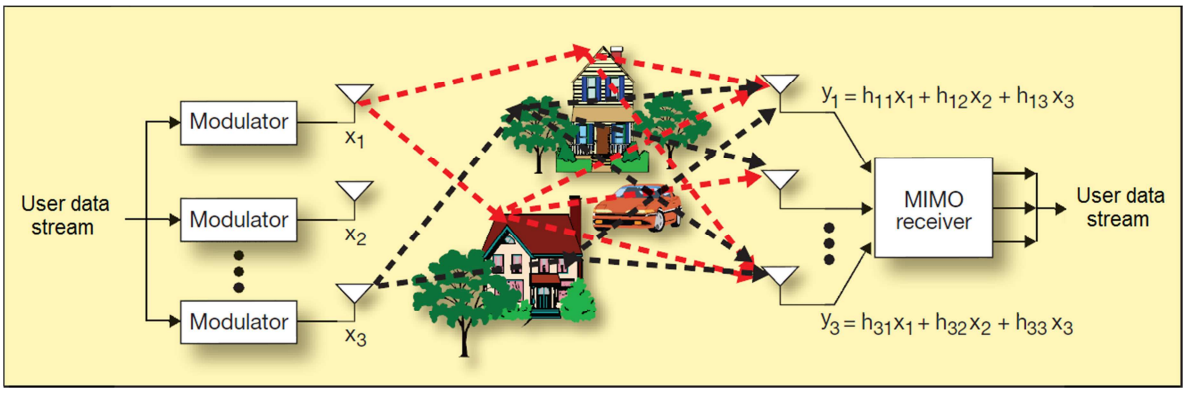

Figure 1.1 MIMO transmission and reception in a dispersive environment. In a MIMO system, different information is transmitted simultaneously on each transmit antenna.

The coefficients *{hij}* represent the channel weights corresponding to the attenuation seen between each transmit-receive antenna pair. The effect is that we have a system of three equations and three unknowns as shown below

$$\mathbf{y} = H \begin{bmatrix} x_1 \\ x_2 \\ x_3 \end{bmatrix}. \tag{1.1}$$

In general, in a system with *M*-transmit antennas and *K*-receive antennas, the channel is characterized by its $K \times M$ channel matrix *H*, of channel coefficients *{hij}*, that must be invertible for MIMO systems to live up to their promise. It has been proven that the likelihood for *H* to be invertible increases as the number of multipaths and reflections in the vicinity of the transmitter or receiver increases. The impact of this is that in a Rayleigh fading environment with spatial independence, there are essentially *MK* levels of diversity available and there are $\min(M, K)$ independent parallel channels that can be established. Increases in the diversity order results in significant reductions in the total transmit power for the same level of performance. On the other hand, an increase in the number of parallel channels translates into an increase in the achievable data rate within the same bandwidth. Let us now quantify the benefits of MIMO-based systems operating in a typical Rayleigh fading wireless channel. Figure 1.2 compares the achievable 95-percentile capacity (minimum capacity achieved over 95 percent of wireless channels encountered, or in other words, given a channel, there is a 95 percent chance that the capacity of that channel is higher than the capacity shown in the plot) for single antenna systems (yellow dot), for a phased array multi-antenna system (blue curve), and for MIMO systems (red curve).

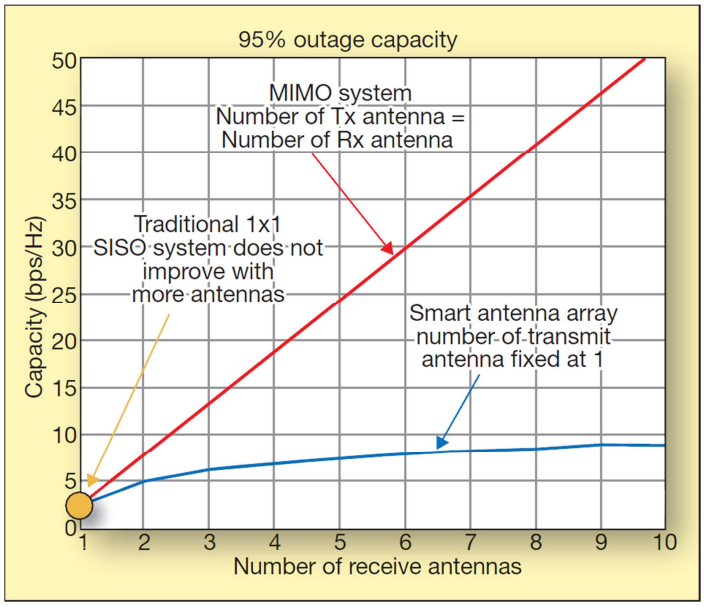

Figure 1.2 MIMO capacity increases with array size, whereas phased array smart antenna systems only improve logarithmically

As shown, the capacity of the phased array system grows logarithmically with increasing antenna array size, whereas the capacity of the MIMO system grows linearly. With four antennas, the phase array system provides a capacity of 8 bps/Hz, whereas the MIMO system provides a capacity of 19 bps/Hz. It is also worth noting that in a phased array system, the array coefficients must be calculated to point the beam in the "best direction". MIMO systems do not suffer from this problem as the geometry of the environment and position of the reflectors are automatically taken into account during the decoding of the MIMO signal. The benefits of MIMO will now be considered in a different light. Assume that there is a fixed capacity that is desired, say 1 bps/Hz, and ask the question, "How much total transmit power is needed to achieve a 95-percentile capacity of 1 bps/Hz?". The results are summarized in Table 1.1.

Antenna Configuration	MIMO
SISO (1 × 1)	12.8 dB
2 × 2	1.2 dB
3 × 3	-4.9 dB
4 × 4	-9.3 dB

Table 1.1 Receive SNR required to achieve a 95-percentile capacity of 1 bps/Hz

As is seen from the table, as the numbers of antennas increase in a MIMO system, less and less receive power is needed to achieve the same data throughput rate. So if a conventional single antenna system required 1 W of transmit power to achieve a certain throughput, then an 8×8 MIMO system would require only 6 mW of power to achieve the same performance.

1.2 A multiplicity of MIMO modes

The appeal of spatial multiplexing MIMO systems has captured many people's attention. This has been taken to the extreme whereby spatial multiplexing MIMO schemes have been suggested to solve any and all wireless communication issues. In fact, there are four unique multi-antenna MIMO techniques available to the system designer as follows:

- Spatial multiplexing (SM-MIMO): In SM systems multiple antennas are used to transmit independent and separately encoded signals, so-called *streams*, from each of the multiple transmit antennas. As such SM-MIMO can result in much improved throughput without increasing bandwidth. The downside to SM is the need for highly complex matrix inversion operations in the receiver, and the added sensitivity to impairments when the system is driven into "full-multiplexing" (number of spatial streams is equal to the number of transmit antennas which in turn is equal to the number of receive antennas) mode of operation.

- Space-time coding (STC-MIMO): Space-time coding rely on transmitting multiple, redundant copies of a data stream to the receiver in the hope that at least some of them may survive the physical path between transmission and reception in a good enough state to allow reliable decoding. Compared to spatial multiplexing systems, STC-MIMO systems provide robustness of communications without providing significant throughput gains. Moreover, they are well suited to asymmetric situations where the transmitter may have more antennas at its disposal than the receiver.

- Diversity systems (DIV-MIMO): Diversity is a traditional form of multi-antenna processing that looks to counteract fast fading effects by creating independent channels between the TX and RX, transmitting the same signal on all independent channels and optimally combining the received signals.

- Smart antenna (SA-MIMO): These systems are best described as adaptive phased array antenna systems that can adaptively beam-form or beam-null in a particular direction.[2]

[2] Beamforming is a signal processing technique used in sensor arrays for directional signal transmission or reception. This spatial selectivity is achieved by using adaptive or fixed receive/transmit beam-patterns. The improvement compared with an omnidirectional reception/transmission is known as the receive/transmit gain (or loss).

Chapter 2

THE VECTOR PERTURBATION TECHNIQUE [2], [3], [12]

2.1 Vector-Perturbation in MIMO systems

Current information theoretic interest in MIMO communications has shifted, in part, away from point-to-point links and into multiuser (or "broadcast") links. Many of the advantages of using multiple antennas in a single-user scenario also translate to large gains in multi-user scenarios. We are interested to find simple techniques to achieve this multi-user gain. It is well known that the point-to-point capacity of M-transmit, N-receive antenna link grows linearly in a Rayleigh fading environment, with the minimum of M and N when the receiver knows the channel. We also know that K users, each with one antenna, can transmit to a single receiver with M antennas and the sum-capacity (total of transmission rates from all K users) grows linearly with the minimum of M and K. It has been more recently shown that this "uplink" transmission has a symmetric "downlink" where the M antennas are used to transmit to the K users; the sum-capacity grows linearly with $\min(M, K)$, provided the transmitter and receivers all know the channel. This particular use of multiple antennas to communicate with many users simultaneously is especially appealing in wireless local area network (WLAN) environments such as IEEE 802.11 and other time-division duplex (TDD) systems where channel conditions can readily be learned by all parties. Some multi-antenna multiuser concepts have also been applied to digital subscriber line (DSL) services, where many twisted pairs of telephone lines are bundled together in one cable leading to interference between users. We are interested primarily in designing a coding technique for the downlink, where an access point (or base-station, or telephone switch) with M antennas (or a bundle of M wires) wants to communicate simultaneously with K users.

To date, schemes to achieve the sum-capacity in these multi-antenna links are largely information-theoretic and rely on layered applications of "dirty paper coding" and interference cancellation. Dirty paper coding is first described for the Gaussian interference channel by Costa [1], where he finds that the capacity of an interference channel where the interfering signal is known at the transmitter (but not necessarily under its control) is the same as the channel with no interference. Costa envisioned the interference as dirt and his signal as ink; his information-theoretic solution is not to oppose the dirt, but to use a code that aligns itself as much as possible with the dirt. Dirty-paper techniques are natural candidates for achieving sum-capacity in multi-antenna multi-user links because the transmitted signal for one user can be viewed as interference for another user, and this interference is known to the transmitter (the transmitter knows everybody's channel). However, it has not been shown that dirty paper coding is necessary for achieving the majority of the capacity. Unlike Costa's original premise that the transmitter knows the interference but cannot control it, in our scenario the

transmitter creates all of the signals, and thereby can also control the interference seen by all the users.

A suitably modified form of channel inversion can achieve near-sum-capacity performance. Channel inversion is one of the simplest modulation techniques for the multi-user channel. This technique multiplies the vector-signal to be transmitted by the inverse of the channel matrix; the result is an "equalized" channel to each user. In the first part it shown that the sum-rate for channel inversion (sometimes also referred to as "zero-forcing (ZF) beamforming") in its plain form is poor. The authors of the technique develop a regularized form of inversion that improves performance, especially at low SNRs, and then they find the regularization parameter that maximizes the signal to interference plus noise ratio (SINR) at each receiver. While regularization improves performance significantly, especially at low SNRs, another step is still needed to obtain near-capacity performance: vector perturbation technique that is used in conjunction with regularization to obtain good performance at all SNRs. The authors modify the data that is transmitted by judiciously adding an integer vector offset. An important data-modifying technique originally developed for the intersymbol interference (ISI) channel is Tomlinson–Harashima (TH) precoding [4], [5]. This technique applies a scalar integer offset at the transmitter that allows cancellation of the interference after application of a modulo function at the receiver. A technique related to both TH precoding and channel inversion can achieve near-sum-capacity even at high SNR, with each user receiving $1/K$ th of the sum-capacity. The following method does not require explicit dirty paper techniques. In fact, while the technique requires the transmitter to know the channel, each receiver needs to know only a single prearranged scalar related to the SNR of the channel.

The method requires the joint selection of a *vector* perturbation of the signal to be transmitted to all the receivers. In general, techniques such as the Fincke–Pohst algorithm [6], [7] (which in our context, we label "sphere encoding"), can aid in selecting the desired vector perturbation. In all cases, however, the processing at the receiver is simple.

2.2 The model

A general model for the forward link of a multiuser system includes an access point with M transmits antennas and K users, each with one receive antenna. The received data at the k^{th} user is

$$y_k = \sum_{m=1}^{M} h_{k,m} x_m + w_k \tag{2.1}$$

where $h_{k,m}$ is the zero-mean unit-variance complex Gaussian fading gain between transmit antenna m and user k, x_m is the signal sent from the m^{th} antenna, and w_k is standard complex Gaussian receiver noise at the k^{th} user. The corresponding vector equation is

$$\mathbf{y} = H\mathbf{x} + \mathbf{w} \tag{2.2}$$

where $\mathbf{y} = [y_1, \dots, y_K]^T$ represents the received signals for each users, $\mathbf{x} = [x_1, \dots, x_M]^T$ denotes the normalized transmitted signals with a power constraint $\mathrm{E}\|\mathbf{x}\|^2 = 1$, and $\mathbf{w} = [w_1, \dots, w_K]^T$ represents the additive white Gaussian noise (AWGN) with covariance matrix $\mathrm{E}[\mathbf{w}\mathbf{w}^*] = \sigma^2 I$. The $K \times M$ matrix H has $h_{k,m}$ as elements

$$H = \begin{bmatrix} h_{1,1} & \dots & h_{1,M} \\ \vdots & \ddots & \vdots \\ h_{K,1} & \dots & h_{K,M} \end{bmatrix}.$$

It is often convenient to construct an unnormalized signal $\mathbf{s}$, such that

$$\mathbf{x} = \frac{\mathbf{s}}{\sqrt{\gamma}} \tag{2.3}$$

where $\gamma = \|\mathbf{s}\|^2$. With this normalization, $\mathbf{x}$ obeys $\|\mathbf{x}\|^2 = 1$. We can, alternatively, let

$$\mathbf{x} = \frac{\mathbf{s}}{\sqrt{\mathrm{E}[\gamma]}}. \tag{2.4}$$

In this case, $\mathrm{E}\|\mathbf{x}\|^2 = 1$. Equation (2.3) has the advantage that $\mathrm{E}[\gamma]$ does not need to exist (we see later that in simple channel inversion, $\mathrm{E}[\gamma] = \infty$), but has the disadvantage that the receivers generally need to know γ, a channel-and data-dependent quantity, to decode their data properly. In the normalization (2.4), the receiver needs to know only $\mathrm{E}[\gamma]$, which is neither channel nor data dependent. Although it is more practical to use (2.4) (when it exists), we choose, for convenience, in most of the simulations to use the instantaneous power normalization (2.3). A discussion of the expected performance difference of using (2.3) versus (2.4) may be found in Section 2.8. Generally, we find that the performance difference to be very small. The simulations, therefore, represent the performance of either normalization, and we assume that the receivers need to know only $\mathrm{E}[\gamma]$.

We concentrate on the scenario where all K users are serviced at the same rate, and assume that H is constant for some interval long enough for the transmitter to learn and use it until it changes to a new value. We are interested in the behavior of the system (2.2), its capacity, and the algorithms to achieve capacity. Many of our theoretical results are obtained for large M and K limits, because the limiting results are often tractable. Nevertheless, we often consider M as small as four in our examples.

An important figure of merit for (2.2) is the ergodic sum capacity

$$C_{\mathrm{sum}} = \mathrm{E}[\sup_{D \epsilon \mathcal{A}} \log_2 |I_M + \rho H^* D H|]. \tag{2.5}$$

Where I_M is the $M \times M$ identity matrix, $\mathcal{A}$ is the set of $K \times K$ diagonal matrices with nonnegative elements, such that $\mathrm{tr}(D) = 1$, and we define $\rho = 1/\sigma^2$. The Hermitian transpose (conjugate

transpose) of H is denoted H^*. We assume the logarithm is base-two and therefore C_{sum} is measured in bits/channel use. Although the total transmitted power is one, the quantity ρ is directly related to, but is not necessarily the same as, the SNR at each receiver.

By simply choosing $D = (1/K)I_K$, we can easily infer that C_{sum} grows linearly with $\min(M, K)$. The expectation in equation (2.5) assumes that coding is done over multiple intervals with independent H. The maximization in (2.5) has no simple closed-form solution, so the authors compute (2.5) numerically using a gradient-type method as needed, but we omit the details from our discussion.

When $K < M$, the optimization over $D \epsilon \mathcal{A}$ given in (2.5) gives nonzero energy to all K users when ρ is large enough. This occurs because omitting any user by setting any diagonal entry of D to zero gains signal energy for the remaining users (which has a logarithmic effect) but loses a transmission degree of freedom (DOF) (which has a more dramatic linear effect). On the other hand, when $K > M$, we know from the formula (2.5) that although transmitting to at least M out of the K users simultaneously uses all of our available DOFs, we may gain by judiciously choosing a subset of fewer than all K users. We do not pursue the choice of subset here; in the interests of fairness to all users, we assume that a random choice of M users is made. In this study, we therefore generally consider the case $K = M$ to be most important.

In (2.2) the users all have the same average (but not instantaneous) received signal power, so our model assumes that the users are similar distances from the access point and are not in deep shadow fades. We also comment that the forward-link problem we are considering needs a fundamentally different solution than the reverse-link problem. In the reverse link, the K users are transmitting simultaneously to the access point that is now acting as the receiver. The reverse link problem has readily available solutions. It is known that it is optimal for the K users to use independent code books, subject to their own power constraints; the receiver can use many forms of decoding such as successive nulling/canceling or maximum-likelihood with reduced complexity (using the sphere decoder). We therefore omit considerations of the reverse link.

2.3 Channel Inversion: some old and new results

2.3.1 An old result (K<M)

Channel inversion, when done at the transmitter, is sometimes known as ZF precoding, and entails deciding that the symbols $\{u_1, \dots, u_K\}$ seen at receivers 1,…,K should be chosen independently, according to the independent data desired for users 1,…,K. We assume that the entries of the vector $\mathbf{u} = [u_1, \dots, u_K]^T$ are chosen from the same constellation with $\mathrm{E}|u_k|^2 = 1$ (ensuring equal rate to the users), and the transmitter then sets

$$\mathbf{s} = H^*(HH^*)^{-1}\mathbf{u}. \tag{2.6}$$

Generally, the inverse in (2.6) can be done only when $\beta = M/K \geq 1$. In this case, the asymptotic (as M and K go to infinity in this fixed ratio) sum rate of channel inversion is

$$\lim_{\{M,K\}\to\infty} \frac{C_{\text{ci}}}{M} = \frac{1}{\beta}\log\big(1+\rho(\beta-1)\big). \tag{2.7}$$

Let $\beta_0 = \beta_0(\rho)$ be the β that maximizes (2.7). Then $\beta_0 > 1$ is the optimum antenna/user ratio, and at this ratio, we can get to within roughly 80% of C_{sum} (2.5) computed at the same ratio. However, at other ratios, the difference between C_{ci} and C_{sum} can become much more pronounced. For example, we see that as $\beta \to 1$, we have $C_{\text{ci}}/M \to 0$. The implication is that for $K = M$, the sum rate of raw channel inversion does not increase linearly with K (or M), while C_{sum} clearly does. We analyze this shortcoming more closely in the next section.

2.3.2 A new result (K=M)

When $K = M$, channel inversion (2.6) becomes simply

$$\mathbf{s} = H^{-1}\mathbf{u}. \tag{2.8}$$

This equation can obviously be problematic when H is poorly conditioned[3], and this problem manifests itself in the normalization constant (2.3)

$$\gamma = \|\mathbf{s}\|^2 = \mathbf{u}^*(HH^*)^{-1}\mathbf{u}. \tag{2.9}$$

Let the entries of $\mathbf{u}$ be zero-mean unit-variance independent complex Gaussian random variables. Then γ has density

$$p(\gamma) = K\frac{\gamma^{K-1}}{(1+\gamma)^{K+1}}. \tag{2.10}$$

A preview of the poor performance of channel inversion can be gleaned by observing that this density has infinite mean $\mathrm{E}[\gamma] = \infty$. The received data at the k^{th} user is

$$y_k = \frac{u_k}{\sqrt{\gamma}} + w_k. \tag{2.11}$$

The receivers all know γ, and we assume that K is large enough so that any user's data does not significantly affect the value of γ. Then, conditioned on γ, the channel becomes a scaled Gaussian channel; the capacity of this channel is

$$C_{\text{ci},k} = \mathrm{E}\left[\log\left(1+\frac{\rho}{\gamma}\right)\right] = \int_0^\infty \log\left(1+\frac{\rho}{\gamma}\right) K\frac{\gamma^{K-1}}{(1+\gamma)^{K+1}}\,d\gamma. \tag{2.12}$$

A change of variables yields

$$C_{\text{ci},k} = \int_0^\infty \log\left(1+\frac{\rho\gamma}{K}\right)\frac{1}{\left(\frac{\gamma}{K}+1\right)^{K+1}}\,d\gamma. \tag{2.13}$$

[3] For square matrices we can measure the sensitivity of the solution of the linear algebraic system $A\boldsymbol{x} = \boldsymbol{b}$ with respect to changes in vector **b** and in matrix A by using the notion of the condition number of matrix A. Condition number is defined as the product of the norm of A and the norm of A-inverse: $\kappa(A) = \|A\|\|A^{-1}\|$. If it is close to one, the matrix is *well conditioned* which means its inverse can be computed with good accuracy. If the condition number is large, then the matrix is said to be *ill-conditioned*. It gives an indication of the accuracy of the results from matrix inversion and the linear equation solution.

Using the large K approximation $1/((\gamma/K+1)^{K+1}) \sim e^{-\gamma}$ in (2.13) (we omit the technical details showing that this substitution is valid in the integral) gives

$$C_{\text{ci},k} \approx \int_0^\infty \log\left(1+\frac{\rho\gamma}{K}\right) e^{-\gamma} d\gamma = e^{\frac{K}{\rho}} E_1\left(\frac{K}{\rho}\right) \log e \tag{2.14}$$

where

$$E_1(x) = \int_x^\infty \frac{e^{-t}}{t} dt \tag{2.15}$$

is the exponential integral. Since there are K users, each with receive (2.11), the sum rate for channel inversion is approximated for large $K = M$ by

$$C_{\text{ci}} \approx K e^{\frac{K}{\rho}} E_1\left(\frac{K}{\rho}\right) \log e \text{ [bits per channel use].} \tag{2.16}$$

We finally use the approximation $E_1(x) \sim e^{-x}/x$ for large x to conclude that

$$\lim_{K\to\infty} C_{\text{ci}} = \rho \log e \text{ [bits per channel use].} \tag{2.17}$$

The unfortunate conclusion is that the sum rate for $K = M$ users with channel inversion is constant as a function of K, as $K\to\infty$. This is in contrast to (2.5), which grows linearly with K. An explanation for this poor capacity comes from looking at the eigenvalues of $(HH^*)^{-1}$ (or singular values of H^{-1}). The smallest eigenvalue of HH^* has distribution $p(\lambda) = Ke^{-K\lambda}$, which is an exponential distribution. The largest eigenvalue of $(HH^*)^{-1}$ therefore has the distribution

$$p(\mu) = \left(\frac{K}{\mu^2}\right) e^{-\frac{K}{\mu}} \tag{2.18}$$

which is sometimes called the *inverse-gamma* distribution with parameter one. This density is zero at $\mu = 0$, but decays as $1/\mu^2$ as $\mu\to\infty$ for any K. Hence, it is a long-tailed distribution with infinite mean. It turns out that the remaining $K-1$ eigenvalues of $(HH^*)^{-1}$ are significantly better behaved.

See Figure 2.1 for a numerical comparison of the largest four eigenvalues of $(HH^*)^{-1}$ as a function of K. In fact, the smallest eigenvalue of $(HH^*)^{-1}$ concentrates (probabilistically) around $1/(4K)$ as $K\to\infty$. Therefore, any approach to improve channel inversion must seek to reduce the effects of the largest eigenvalue.

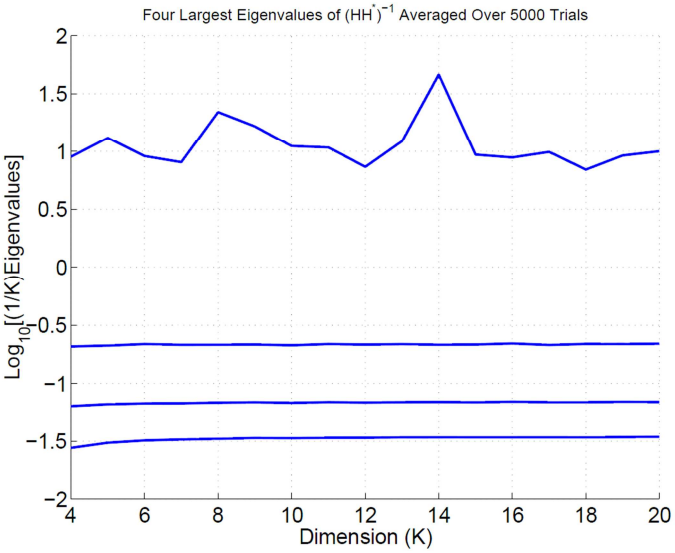

Figure 2.1 Numerical comparison of the mean behavior of the four largest eigenvalues of $(HH^*)^{-1}$ as a function of K. The figure was generated using 5000 trials, and the eigenvalues are normalized by K. The largest eigenvalue has an erratic plot because its true mean is infinite (for all K), and it is clearly orders of magnitude larger than the remaining eigenvalues.

Figure 2.2 shows the sum rate for channel inversion evaluated numerically, the large-K expression (2.17) and the sum capacity (2.5). We can see that as the number of transmit antennas and users grow simultaneously, the sum rate for channel inversion approaches, while the sum capacity grows linearly.

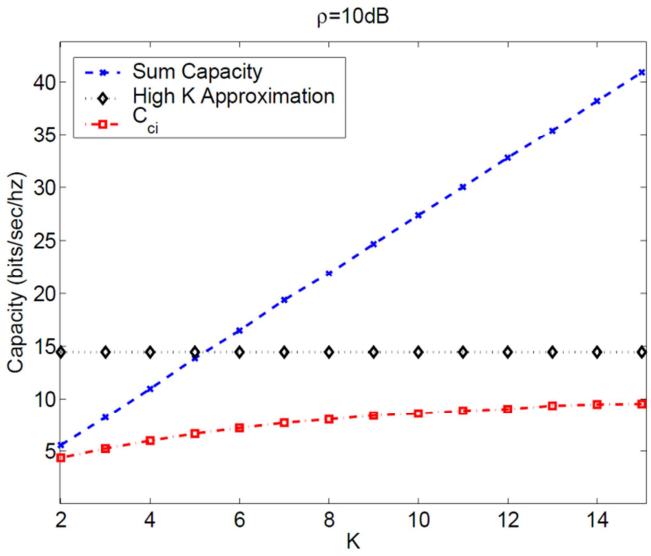

Figure 2.2 Comparison of the sum capacity (2.5) (blue line) as a function of K for $\rho = 10$ dB, with the channel-inversion sum rate (K times the value in (2.12)) (red line). Rather than growing linearly, C_{ci} approaches the large-K limit (2.17), which is shown as a black line.

We assume that $K = M$ in the remainder of this study.

2.4 Regularizing the inverse

One technique often used to "regularize" an inverse is to add a multiple of the identity matrix before inverting. For example, instead of forming $\mathbf{s}$ using (2.8), we use

$$\mathbf{s} = H^*(HH^* + \alpha I_K)^{-1}\mathbf{u}. \tag{2.19}$$

After going through the channel, the unnormalized signal $\mathbf{s}$ becomes

$$H\mathbf{s} = HH^*(HH^* + \alpha I)^{-1}\mathbf{u}. \tag{2.20}$$

The signal received at user k is no longer simply a scaled version of u_k, but also includes some "crosstalk" interference from the remaining users.

To evaluate the amount of desired signal and interference, it use the eigenvalue decomposition $HH^* = Q\Lambda Q^*$ for nonnegative diagonal eigenvalue matrix Λ and unitary eigenvector matrix Q to find

$$H\mathbf{s} = Q\frac{\Lambda}{\Lambda + \alpha \mathrm{I}}Q^*\mathbf{u}. \tag{2.21}$$

(We use the convention that commuting matrices can be treated as scalar, and therefore, may appear in fractional form.) The (unnormalized) signal and interference received by user k is the k^{th} entry of $H\mathbf{s}$. Using (2.21), we may find this entry

$$[H\mathbf{s}]_k = \begin{bmatrix} q_{k,1}\dfrac{\lambda_1}{\lambda_1+\alpha} & \cdots & q_{k,K}\dfrac{\lambda_K}{\lambda_K+\alpha} \end{bmatrix} \begin{bmatrix} q_{1,1}^* & \cdots & q_{K,1}^* \\ \vdots & \ddots & \vdots \\ q_{1,K}^* & \cdots & q_{K,K}^* \end{bmatrix} \begin{bmatrix} u_1 \\ \vdots \\ u_K \end{bmatrix} \tag{2.22}$$

where $q_{k,l}$ is the $(k,l)^{\text{th}}$ entry of the matrix Q. The (unnormalized) desired signal term in (2.22) is

$$\left(\sum_{l=1}^{K}\frac{\lambda_l}{\lambda_l+\alpha}\left|q_{k,l}\right|^2\right)u_k. \tag{2.23}$$

All the remaining terms in (2.22) involving u_l $(l \neq k)$ are interference. The k^{th} user models its (normalized) received signal as

$$y_k = \left(\frac{1}{\sqrt{\gamma}}\right)\left(\sum_{l=1}^{K}\frac{\lambda_l}{\lambda_l+\alpha}\left|q_{k,l}\right|^2\right)u_k + w_k' \tag{2.24}$$

where the Gaussian w_k' combines the additive receiver noise w_k and the interference. The receiver makes its decisions about the transmitted signal by forming the likelihood function from (2.24). The amount of interference is determined by $\alpha > 0$; when $\alpha = 0$, we return to (2.8). It is clear that, no matter how poorly conditioned H is, the inverse in (2.19) can be made to behave as well as desired by choosing α large enough. We examine the optimum value of α to choose. The amount of interference increases with α, so one possible metric for choosing α is to maximize the SINR in (2.24). We compute the SINR by computing the expected power of the desired signal and dividing it by the expected power of the interference plus noise.

The noise power at each receiver is given by σ^2.

From (2.2), the signal (without noise) observed at the K receivers is $H\mathbf{x} = \left(1/\sqrt{\mathrm{E}[\gamma]}\right)H\mathbf{s}$ (we assume that the average power normalization (2.4) is used). We need to examine the relative strengths of the desired signal and interference at each receiver; we first examine the behavior of $\gamma = \|\mathbf{s}\|^2$.

We use the eigenvalue decomposition of HH^* to obtain

$$\begin{aligned}\gamma &= \mathbf{u}^*(HH^*+\alpha I)^{-1}HH^*(HH^*+\alpha I)^{-1}\mathbf{u}\\ &= \mathrm{tr}[(Q\Lambda Q^*+\alpha I)^{-1}Q\Lambda Q^*(Q\Lambda Q^*+\alpha I)^{-1}\mathbf{u}\mathbf{u}^*]\\ &= \mathrm{tr}[Q(\Lambda+\alpha I)^{-1}Q^*Q\Lambda Q^*Q(\Lambda+\alpha I)^{-1}Q^*\mathbf{u}\mathbf{u}^*]\\ &= \mathrm{tr}\left[\frac{\Lambda}{(\Lambda+\alpha I)^2}Q^*\mathbf{u}\mathbf{u}^*Q\right].\end{aligned}$$

We assume that the data $u_1,\ldots,u_K$ are independently chosen with zero-mean and unit-variance. Taking the conditional expectation of γ with respect to $\mathbf{u}$ and using $\mathrm{E}[\mathbf{u}\mathbf{u}^*] = I_K$, we get

$$\mathrm{E}[\gamma] = \mathrm{tr}\left[\frac{\Lambda}{(\Lambda+\alpha I)^2}\right] = \sum_{l=1}^{K}\frac{\lambda_l}{(\lambda_l+\alpha)^2}. \tag{2.25}$$

It's convenient to take expectations only with respect to $\mathbf{u}$ and Q when evaluating the quantities needed to compute the SINR. The expectations with respect to Λ are generally difficult. It shows later that, fortunately, the final result does not require taking the expectation with respect to Λ. From (2.21), the total expected power in $H\mathbf{s}$ is

$$\mathrm{E}\|H\mathbf{s}\|^2 = \mathrm{E}\left[\mathbf{u}^* Q \left(\frac{\Lambda}{\Lambda + \alpha I}\right)^2 Q^* \mathbf{u}\right] = \sum_{l=1}^{K} \frac{\lambda_l^2}{(\lambda_l + \alpha)^2}. \tag{2.26}$$

Was still avoided the expectation with respect to Λ. The desired signal for the k^{th} user is given by (2.23). To find the expectation power of the signal, it computes the expectation over Q in [2], using the fact that Q and Λ are statistically independent

$$\text{Desired} = \mathrm{E}\left[\left(\sum_{l=1}^{K} \frac{\lambda_l}{\lambda_l + \alpha} |q_{k,l}|^2\right)^2\right] = \frac{1}{K(K+1)}\left[\left(\sum_{l=1}^{K} \frac{\lambda_l}{\lambda_l + \alpha}\right)^2 + \sum_{l=1}^{K}\left(\frac{\lambda_l}{\lambda_l + \alpha}\right)^2\right]. \tag{2.27}$$

This is the unnormalized power of the desired signal at the receiver. Observe that this power is one when α = 0 (plain channel inversion). The normalized power divides (2.27) by E[γ]. The total signal and interference power at any receiver is $1/K$ th of the total (unnormalized) power appearing at all the receives (2.26), which is $(1/K)\sum_{l=1}^{K} {\lambda_l}^2/(\lambda_l + \alpha)^2$. Hence, subtracting off the power of the desired signal (2.27) leaves the power of the interference u_l ($l \neq k$) at receiver k as

$$\text{Undesired} = \frac{1}{K}\sum_{l=1}^{K}\left(\frac{\lambda_l}{\lambda_l + \alpha}\right)^2 - \frac{1}{K(K+1)}\left[\left(\sum_{l=1}^{K} \frac{\lambda_l}{\lambda_l + \alpha}\right)^2 + \sum_{l=1}^{K}\left(\frac{\lambda_l}{\lambda_l + \alpha}\right)^2\right]. \tag{2.28}$$

This is the unnormalized power of the interference at each receiver. Observe that this power is zero when α = 0. The normalized power divides (2.28) by E[γ]. Putting (2.27) and (2.28) together, normalized by γ as given by (2.25), yields

$$\text{SINR} = \frac{\left(\sum_{l=1}^{K} \frac{\lambda_l}{\lambda_l+\alpha}\right)^2 + \sum_{l=1}^{K}\left(\frac{\lambda_l}{\lambda_l+\alpha}\right)^2}{\sigma^2 K(K+1)\sum_{l=1}^{K} \frac{\lambda_l}{(\lambda_l+\alpha)^2} + K\sum_{l=1}^{K}\left(\frac{\lambda_l}{\lambda_l+\alpha}\right)^2 - \left(\sum_{l=1}^{K} \frac{\lambda_l}{\lambda_l+\alpha}\right)^2}. \tag{2.29}$$

Because of the symmetry in the distribution of H, (2.29) is not a function of the user k. Rather than optimize (2.29) directly over α, it prefers to optimize a simpler large-K approximation to (2.29). The large-K approximation follows from removing the second summation in the numerator of (2.29), which is dwarfed by the first summation, and replacing $K(K+1)$ by K^2. We then obtain

$$\text{SINR} \approx \frac{\left(\sum_{l=1}^{K} \frac{\lambda_l}{\lambda_l+\alpha}\right)^2}{\sigma^2 K^2 \sum_{l=1}^{K} \frac{\lambda_l}{(\lambda_l+\alpha)^2} + K\sum_{l=1}^{K}\left(\frac{\lambda_l}{\lambda_l+\alpha}\right)^2 - \left(\sum_{l=1}^{K} \frac{\lambda_l}{\lambda_l+\alpha}\right)^2}. \tag{2.30}$$

Remarkably, the large-K approximation (2.30) in maximized for $\alpha \geq 0$ at $\alpha_{\text{opt}} = K\sigma^2 = K/\rho$, *independently of* $\lambda_1, \ldots, \lambda_K$. For a proof, consult [2]. Simulations indicate that (2.30) is close to the true SINR, for even small values of K; α_{opt} is proportional to K and the noise variance. As we decrease the noise variance at each receiver, thereby increasing the SNR, $\alpha_{\text{opt}} \to 0$.

The above analysis only uses the fact that the eigenvector matrix Q has the so-called isotropic distribution, whose defining characteristic is that pre-or-post multiplying Q by any unitary matrix does not affect its distribution. Physically, this means that the channel is not affected by arbitrary rotations, and that paths between the antennas and the users are statistically equivalent. It is this feature that allows us to examine the SINR of any user and claim that this analysis applies equally to the remaining users. This analysis, therefore, applies to other channel distributions with this rotational-invariance property, and not just a Gaussian H.

2.5 Performance and capacity

Three figures show the trends in performance. Figure 2.3 shows the symbol-error probability (SEP) for plain and regularized channel inversion as a function of ρ for $K = 4$ and $K = 10$. The curves indicate that while the performance of plain channel inversion worsens with K, the performance of regularized inversion improves slightly with K.

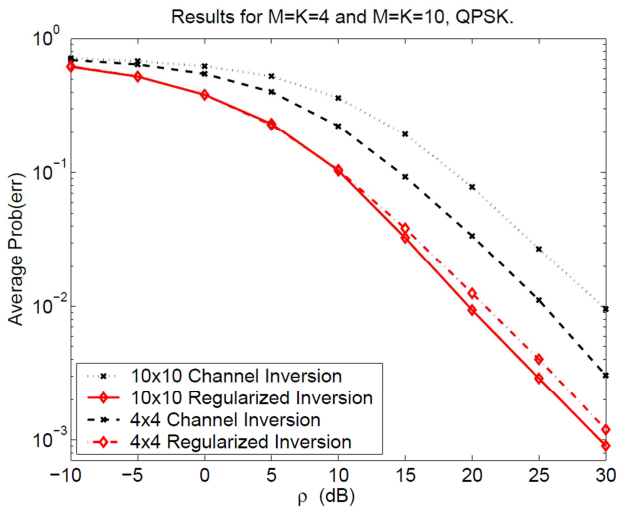

Figure 2.3 Comparison of the SEP for plain (2.8) and regularized (2.19) channel inversion for $K = 4$ and $K = 10$. The raw error rate as a function of K worsens for plain channel inversion, but improves (slightly) for regularized inversion.

A comparison of the sum capacity and sum rates for regularized and plain channel inversion as a function of K is shown in Figure 2.4. The sum rate for regularized channel inversion is obtained using a numerical estimate of the SINR with $\alpha = K/\rho$

$$C_{\text{reg}} \approx K \log(1 + \text{SINR}). \tag{2.31}$$

Unlike channel inversion, the sum rate of regularized inversion has growth with K, although its slope is different from the sum capacity.

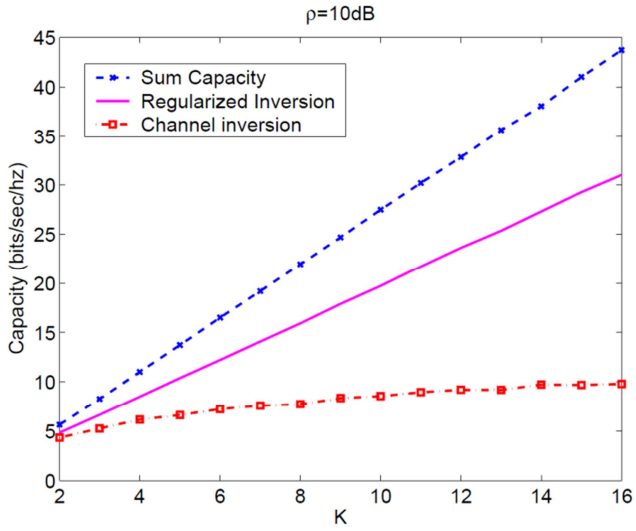

Figure 2.4 Comparison of the sum capacity (2.5) (blue line) as a function of K (where $M = K$) for $\rho = 10$ dB, with the regularized channel-inversion sum rate (2.31) (purple line) and the plain channel-inversion sum-rate (red line). Unlike plain channel inversion, regularized inversion has linear growth with K.

Figure 2.5 shows that for a fixed K, as $\rho \to \infty$ ($\sigma^2 \to 0$), the sum rate of regularized inversion approaches plain inversion $C_{\text{reg}} \to C_{\text{ci}}$. Thus, we still do not have a modulation technique which is close to capacity for all ρ and K.

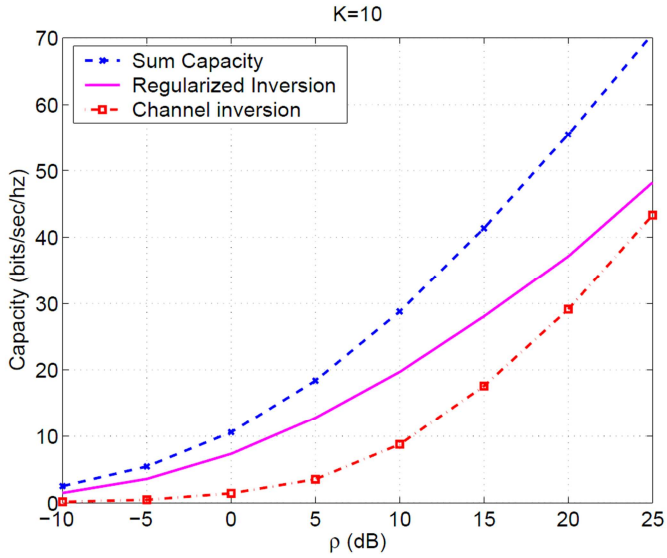

Figure 2.5 Comparison of sum capacity (2.5) (blue line) as a function of ρ for $K = M = 10$, with the regularized channel-inversion sum rate (2.31) (purple line) and the plain channel-inversion sum rate (red line). At low power, regularized inversion approaches C_{sum}, while for high ρ, it approaches C_{ci}.

These three figures show that although regularization is a big improvement over plain inversion, a gap to capacity remains, especially at high SNR. This gap is dramatically reduced in the next section, which shows how to combine regularization with a carefully chosen integer vector perturbation of the data to be transmitted to reduce the power of the transmitted signal dramatically.

2.6 Perturbing the data

In the previous sections we argue that many of the problems with inverting the channel when $K = M$ are due to the normalization constant γ, which is often very large because of the large singular values in the inverse of the channel matrix H. One way to help H is to regularize its inverse, as described. This section presents a way to "perturb" the data in a data-dependent way (unknown to the receivers). The goal is to form a $\tilde{\mathbf{u}}$ from the data vector $\mathbf{u}$ such that

$$\mathbf{s} = H^{-1}\tilde{\mathbf{u}} \tag{2.32}$$

has norm (much) smaller than $H^{-1}\mathbf{u}$, but the entries of $\tilde{\mathbf{u}}$ can still be decoded individually at the receivers. We cannot, in general, perturb by an arbitrary complex vector, because this perturbation is not known to the receivers and would, therefore, cause decoding errors. We can, however, use an idea derived from TH precoding, where we allow each element of $\mathbf{u}$ to be perturbed by an integer. In the simplest case, we set

$$\tilde{\mathbf{u}} = \mathbf{u} + \tau\boldsymbol{\ell} \tag{2.33}$$

where τ is a positive real number and $\boldsymbol{\ell}$ is a K-dimensional complex vector $a + ib$, where a and b are integers. The scalar $\gamma = \|\mathbf{s}\|^2$ is computed as before, and the transmitted signal is

$$\mathbf{x} = \frac{1}{\sqrt{\gamma}} H^{-1}\tilde{\mathbf{u}}. \tag{2.34}$$

The scalar τ, that is known to the receivers, is chosen large enough so that the receivers may apply the modulo function

$$f_\tau(y) = y - \left\lfloor \frac{y + \tau/2}{\tau} \right\rfloor \tau \tag{2.35}$$

where the function $\lfloor\cdot\rfloor$ is the largest integer less than or equal to its argument. The function (2.35) removes the effect of the integer multiple of τ. (The function $f_\tau(y)$ is applied separately to the real and imaginary components of a complex y.) After passing through the channel H, the transmitted signal $\mathbf{x}$ in (2.34) appears at receiver k as

$$y_k = \frac{1}{\sqrt{\gamma}}\tilde{u}_k + w_k.$$

If we ignore for the moment the effect of w_k, and assume that $\gamma = 1$, then

$$f_\tau(y_k) = f_\tau(u_k + \tau l_k) = u_k$$

and we recover the transmitted symbol. The receivers know γ, and therefore, may compensate for $\gamma \neq 1$ by dividing τ by $\sqrt{\gamma}$. As we note in Section 2.2, the transmitter may instead divide by $\sqrt{\mathrm{E}[\gamma]}$; Figure 2.9 shows that the performance difference is not significant. The other figures assume that the transmitter divides by $\sqrt{\gamma}$. An error is made at the receiver if the additive channel noise pushes the received signal across the standard symbol decoding boundaries or across the nonlinear boundaries of $f_\tau(y)$ at $\pm\tau/2$.

2.6.1 Choice of $\boldsymbol{\ell}$ and τ

An obvious choice of $\boldsymbol{\ell}$ at the transmitter minimizes $\gamma = \|\mathbf{s}\|^2$, in fact if γ is very large the SINR is small and hence overall system performance (error probability) degrades significantly

$$\boldsymbol{\ell} = \arg\min_{\boldsymbol{\ell}'} \gamma = \arg\min_{\boldsymbol{\ell}'} (\mathbf{u} + \tau\boldsymbol{\ell}')^* (HH^*)^{-1} (\mathbf{u} + \tau\boldsymbol{\ell}'). \tag{2.36}$$

This is a K-dimensional integer-lattice[4] least-squares[5] problem, for which there is a large selection of exact and approximate algorithms. See, for example, the Fincke-Pohst algorithm [6], that is used for space-time demodulation in [8], where it is called a *sphere decoder.* Because we are using this algorithm for encoding data to be transmitted, we refer to it as the *sphere encoder*. This algorithm avoids an exhaustive search over all possible integers in the lattices by limiting the search space to a sphere of some given radius centered around a starting point. In our case, the center is the vector $\mathbf{u}$. Generally, the sphere encoder works on real lattices, so we assume that a complex version is used, or that (2.36) has been converted to a $2K$-dimensional real lattice problem.

Various precoding techniques can be interpreted as approximations of (2.36). This includes ZF precoding without perturbation ($\boldsymbol{\ell} = 0$), Tomlinson-Harashima precoding [4], [5], and LR-assisted vector perturbation [11].

The scalar $\tau > 0$ is a design parameter that may be chosen to provide a symmetric decoding region around (the real or imaginary part of) every signal constellation point. It chooses

$$\tau = 2(|c|_{\max} + \Delta/2) \tag{2.37}$$

where $|c|_{\max}$ is the absolute value of the constellation symbol(s) with largest magnitude, and Δ is the spacing between constellation points. If we want to reduce the effects of the perturbation vector $\boldsymbol{\ell}$, we may increase τ, thereby increasing the decoding region at the upper and lower extremes of the constellation. While this improves error performance in these decoding regions, the γ that results is typically also larger, possibly reducing total error performance. If τ is made too large, the minimization in (2.36) yields $\boldsymbol{\ell} = 0$ independently of $\mathbf{u}$, and the perturbation technique reduces to simple channel inversion. If τ is made smaller than $2|c|_{\max}$, then error-free decoding becomes impossible, even in the absence of channel noise. It has found that choosing τ as in (2.37) often works well.

---

[4] The n-dimensional integer-lattice, denoted Z^n, is the lattice in the Euclidean space R^n whose lattice points are n-tuples of integers.

[5] The term least-squares describes a frequently used approach to solving overdetermined or inexactly specified systems of equations in an approximate sense. Instead of solving the equations exactly, we seek only to minimize the sum of the squares of the residuals. It has an important statistical interpretation: if appropriate probabilistic assumptions about underlying error distributions are made, least squares produces what is known as the *maximum-likelihood* estimate of the parameters. Even if the probabilistic assumptions are not satisfied, years of experience have shown that least-squares produces useful results.

2.6.2 Analysis of Vector-Perturbation Technique

As shown in Section 2.3.2, plain channel inversion performs poorly, because $(HH^*)^{-1}$ has a badly behaved large eigenvalue. In this section, we provide a brief theoretical discussion of why using the perturbation vector $\tau\boldsymbol{\ell}$ improves the performance significantly, especially for large K. The discussion is confined to large K, where the analysis is most tractable. The vector $\boldsymbol{\ell}$ is chosen to minimize the norm of $\mathbf{s} = H^{-1}\tilde{\mathbf{u}}$ in (2.32) (using the cost function (2.36)). Using the eigenvalue decomposition $(HH^*)^{-1} = Q\Lambda^{-1}Q^*$, we can express the cost function as

$$\gamma = \|\mathbf{s}\|^2 = \sum_{k=1}^{K} \mu_k \delta_k^2 \tag{2.38}$$

where $\mu_k = 1/\lambda_k$, $\delta_k = |\mathbf{q}_k^* \tilde{\mathbf{u}}|$, and $\mathbf{q}_k$ is the k^{th} column of Q. We assume that $\mu_1 > \mu_2 > \cdots > \mu_k$. The vector-perturbation algorithm minimizes (2.38) over $\tilde{\mathbf{u}}$, where $\tilde{\mathbf{u}} = \mathbf{u} + \tau\boldsymbol{\ell}$, and we search over the integer vector $\boldsymbol{\ell}$. We would like to examine the behavior of $\mathrm{E}[\gamma]$ as a function of K. In 2.3.2, it is shown that $\mathrm{E}[\gamma] = \infty$ for plain (without the perturbation) channel inversion. We argue that with the perturbation, $\mathrm{E}[\gamma]$ is approximately constant with K, and therefore, the sum-rate for the method grows linearly with K.

Recall that τ is chosen large enough so that no element of $\tilde{\mathbf{u}}$ can be made zero. In fact, with our choice of τ, the norm of $\tilde{\mathbf{u}}$ is minimized by choosing $\boldsymbol{\ell} = 0$. Thus, although a nonzero $\boldsymbol{\ell}$ increases the norm of $\tilde{\mathbf{u}}$, the norm of $\mathbf{s} = H^{-1}\tilde{\mathbf{u}}$ is decreased in the process. There is no norm constraint on $\boldsymbol{\ell}$, and hence, the choice of possible points $\tilde{\mathbf{u}}$ form an infinite lattice.

Define

$$\nu = \mathrm{E}\left[\prod_{k=1}^{K} \frac{\delta_k^2}{c^2}\right]^{1/K} \tag{2.39}$$

where

$$c^2 = \frac{\mathrm{E}\|\tilde{\mathbf{u}}\|^2}{K} \tag{2.40}$$

and the expectation is over Q and $\mathbf{u}$. It takes as empirical axiom that ν is positive and approximately independent of K as $K \to \infty$. Equation (2.39) is the expected geometric mean of $\delta_1, \ldots, \delta_K$. The fact that $\nu > 0$ is a consequence of the constraints on $\tilde{\mathbf{u}}$, for if $\tilde{\mathbf{u}}$ is unconstrained, then $\nu = 0$ (the minimizer of (2.38) is parallel to $\mathbf{q}_K$, and, therefore, obeys $\delta_1 = \cdots = \delta_{K-1} = 0, \delta_K = \|\tilde{\mathbf{u}}\|$). We contend that forcing $\boldsymbol{\ell}$ to have integer components when minimizing (2.38) does not generally permit $\tilde{\mathbf{u}}$ to be chosen exactly parallel to $\mathbf{q}_K$ (an axis in a random coordinate system), and thus, the $\boldsymbol{\ell}$ that minimizes (2.36) generates a $\tilde{\mathbf{u}}$ that can only be coarsely oriented in the coordinate system defined by $\mathbf{q}_1, \cdots, \mathbf{q}_K$. The orientations with respect to $\mathbf{q}_1, \cdots, \mathbf{q}_K$ do not change significantly with K, and hence, the expected geometric mean of $\delta_1, \ldots, \delta_K$ is approximately independent of K. A similar statement can be made for the expected mean $\delta_1, \ldots, \delta_K$.

Since the columns of Q form an orthonormal basis

$$\sum_{k=1}^{K} \delta_k^2 = \|\tilde{\mathbf{u}}\|^2. \tag{2.41}$$

Combining (2.41) and (2.40), we see that c^2 can also be rewritten

$$c^2 = \frac{1}{K} \mathrm{E}\left[\sum_{k=1}^{K} \delta_k^2\right] \tag{2.42}$$

and is approximately independent of K. Applying the arithmetic-geometric-mean inequality[6]

$$\mathrm{E}[\gamma] = \mathrm{E}\left[\sum_{k=1}^{K} \mu_k \delta_k^2\right] \geq K\mathrm{E}\left[\left(\prod_{k=1}^{K} \mu_k\right)^{1/K} \left(\prod_{k=1}^{K} \delta_k^2\right)^{1/K}\right]. \tag{2.43}$$

It can be shown that $K\left(\prod_{k=1}^{K} \mu_k\right)^{1/K} \to e$ as $K \to \infty$ (observe that no expectation in seeded here). Equation (2.39) implies that $\mathrm{E}\left[\prod_{k=1}^{K} \delta_k^2\right]^{1/K} = \nu c^2$. Therefore, (2.43) becomes

$$\mathrm{E}[\gamma] \geq e\nu c^2. \tag{2.44}$$

By combining (2.44) with (2.42), we also conclude that

$$\mathrm{E}[\gamma] \geq e\nu \frac{\mathrm{E}\|\tilde{\mathbf{u}}\|^2}{K} \tag{2.45}$$

equality in (2.44) and (2.45) is achieved if

$$\mathrm{E}[\mu_1 \delta_1^2] = \cdots = \mathrm{E}[\mu_K \delta_K^2] = \frac{e\nu c^2}{K}. \tag{2.46}$$

Thus, a way to minimize $\mathrm{E}[\gamma]$ is to have the optimum $\tilde{\mathbf{u}}$ orient itself toward each eigenvalue in inverse proportion to the eigenvalue (on average). The values of c and ν are determined by simulation. Observe that the lower bound (2.44), if achievable, suggests that γ is approximately independent of K as $K \to \infty$. It turns out that the vector-perturbation algorithm minimizing (2.36) nearly achieves the lower bound (2.45).

We conclude that optimizing (2.36) tends to generate a $\tilde{\mathbf{u}}$ that, on average, is oriented toward each eigenvalue of $(HH^*)^{-1}$ in inverse proportion to the eigenvalue as in (2.46). The value of γ that results nearly achieves the lower bound (2.45), and is approximately independent of K.

---

[6] The arithmetic mean of a list of n numbers $x_1, \ldots, x_n$ is $\frac{1}{n}\sum_{i=1}^{n} x_i$; the geometric mean is $\sqrt[n]{\prod_{i=1}^{n} x_n}$. The arithmetic-geometric-mean inequality, states that the arithmetic mean of a list of non-negative real numbers is greater than or equal to the geometric mean of the same list; and further, that the two means are equal if and only if every number in the list is the same.

$$\frac{1}{n}\sum_{i=1}^{n} x_i \geq \sqrt[n]{\prod_{i=1}^{n} x_n}$$

2.6.3 Performance with the perturbation

Figure 2.6 provides an uncoded symbol probability of error plot for plain channel inversion, regularized inversion, vector perturbation and a regularized version of the sphere encoder that is presented in Section 2.7. The probability of error is shown for 16-QAM signaling with K = 10 transmit antennas and users, as a function of ρ. Although the vector-perturbation technique does not do as well as the successive algorithm or regularized inversion for low ρ, it achieves a significant gain in performance for high ρ. The regularized perturbation technique described next in section performs well for all ρ. Figure 2.6 shows that the beneficial effect of regularization is generally a gain in ρ, with little effect on the high-ρ slope (or "diversity") of the error curve. The linear inversion-based methods have the lowest diversity. Only the vector-perturbation method retains a high diversity at high ρ.

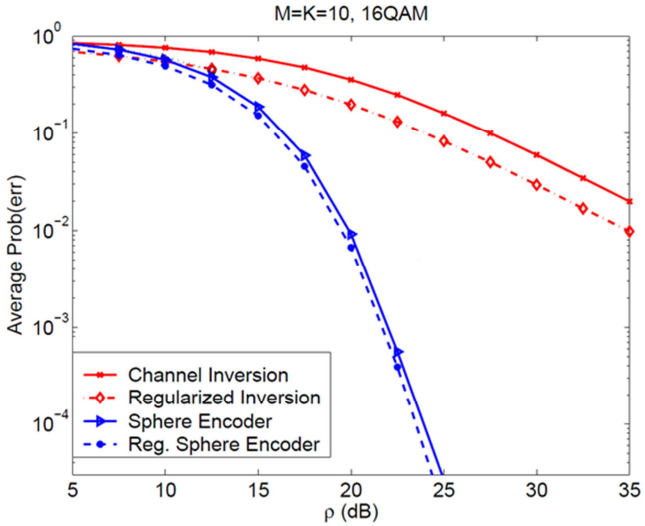

Figure 2.6 Uncoded probability of symbol error for channel inversion (Section 2.3) (x's, solid red line), regularized inversion (Section 2.4) (diamonds, dash-dotted red line), the vector-perturbation algorithm (2.36) (triangles blue line), and the regularized perturbation technique (2.47) (dashed blue line, using $\alpha = 1/\rho$ – see Section 2.7).

2.7 Regularized perturbation

We can marry the regularized inversion method of Section 2.4 with the vector-perturbation technique of Section 2.6 to reduce γ more than either method could alone over a wide range of ρ. The choice of the integer vector $\boldsymbol{\ell}$ that minimizes γ is made with the modified cost function

$$\boldsymbol{\ell} = \arg\min_{\boldsymbol{\ell}'} \|H^*(HH^* + \alpha I_K)^{-1}(\mathbf{u} + \tau\boldsymbol{\ell}')\|^2. \qquad (2.47)$$

Unfortunately, the analysis of the combined method appears to be difficult. In Section 2.4, α is chosen to maximize an approximation to the SINR. The authors do not know how to compute the average SINR after the minimization (2.47), and α_{opt} is generally no longer K/ρ when regularization is combined with perturbation. Because γ is significantly smaller in (2.47) than with regularization alone, $\alpha = K/\rho$ is too large, and gives too much crosstalk from the other users. The optimum α is generally

significantly smaller. For example, probability-of-error simulations show that $\alpha_{\text{opt}} \approx 1/(5\rho)$ for $K = 4$, and $\alpha_{\text{opt}} \approx 1/\rho$ for $K = 10$. The authors do not have a good explanation for these choices, but in the next Section is proposed a systematic manner to find α_{opt}.

2.7.1 Optimizing α

With the regularized perturbation, the received signal can be written as

$$\begin{aligned}\mathbf{y} &= \frac{1}{\sqrt{\gamma}} HH^*(HH^* + \alpha I)^{-1}(\mathbf{u} + \tau\boldsymbol{\ell}) + \mathbf{w} \\ &= \frac{1}{\sqrt{\gamma}}[I - I + (I + \alpha(HH^*)^{-1})^{-1}](\mathbf{u} + \tau\boldsymbol{\ell}) + \mathbf{w} \\ &= \frac{1}{\sqrt{\gamma}}[I(\mathbf{u} + \tau\boldsymbol{\ell}) + A(\mathbf{u} + \tau\boldsymbol{\ell})] + \mathbf{w}\end{aligned} \tag{2.48}$$

where $A = \{(I + \alpha(HH^*)^{-1})^{-1} - I\}$. The received signal for user k is

$$y_k = \frac{[(u_k + \tau\ell_k) + \langle A(\mathbf{u} + \tau\boldsymbol{\ell})\rangle_k]}{\sqrt{\gamma}} + w_k \tag{2.49}$$

where the notation $\langle M\rangle_k$ represents the k^{th} row of the matrix *M.* It is clear that $\langle A(\mathbf{u} + \tau\boldsymbol{\ell})\rangle_k$ is potentially correlated with u_k and ℓ_k. By modeling this correlation, we may model the received signal per user as

$$y_k = \frac{[(u_k + \tau\ell_k) + (\beta_k u_k + \delta_k\tau\ell_k) + v_k]}{\sqrt{\gamma}} + w_k \tag{2.50}$$

where v_k is uncorrelated with u_k and ℓ_k, and β_k and δ_k represent the correlation coefficients of the term $\langle A(\mathbf{u} + \tau\boldsymbol{\ell})\rangle_k$ with u_k and ℓ_k. To solve β_k and δ_k we use the requirements

$$\begin{aligned}\mathrm{E}[v_k u_k^*] &= 0 \\ \mathrm{E}[v_k\tau\ell_k^*] &= 0\end{aligned} \tag{2.51}$$

by defining

$$q_k = \sqrt{\gamma}y_k - (u_k + \tau\ell_k) = \beta_k u_k + \delta_k\tau\ell_k + v_k + \sqrt{\gamma}w_k \tag{2.52}$$

we employ (2.51) to obtain

$$\begin{aligned}\mathrm{E}[q_k u_k^*] &= \beta_k\mathrm{E}[|u_k|^2] + \delta_k\tau\mathrm{E}[\ell_k u_k^*] \\ \mathrm{E}[q_k\tau\ell_k^*] &= \beta_k\tau\mathrm{E}[u_k\tau\ell_k^*] + \delta_k\tau^2\mathrm{E}[|\ell_k|^2].\end{aligned} \tag{2.53}$$

We may solve for β_k and δ_k using these two equations. Generally β_k and δ_k are real, because the real and imaginary parts of the constellation symbols are uncorrelated. The SINR is

$$\text{SINR} = \frac{(1 + \beta_k)^2\,\mathrm{E}[|u_k|^2]/\gamma}{\mathrm{E}\big[[|v_k|^2]\big]/\gamma + \sigma^2}. \tag{2.54}$$

We define the optimum regularization parameter as

$$\alpha_{\text{opt}} = \max_\alpha \text{SINR}. \tag{2.55}$$

The effect of α in SINR is through the normalization factor γ, the correlation β_k, and the variance of v_k. Increasing α generally decreases γ, thus potentially increasing the SINR, but increases the variance of

v_k, thus potentially decreasing the SINR. The overall effect on the SINR is difficult to determine analytically so we use numerical methods. Figure 2.7 shows (2.54) as α is varied from 0 to $2/\rho$ for M = K = 10 and $\rho = 14$ dB. The maximum SINR occurs at $\alpha_{\text{opt}} = 1.2/\rho$, compare $\alpha = 1/\rho$, which minimizes the bit-error-rate in Section 2.7.

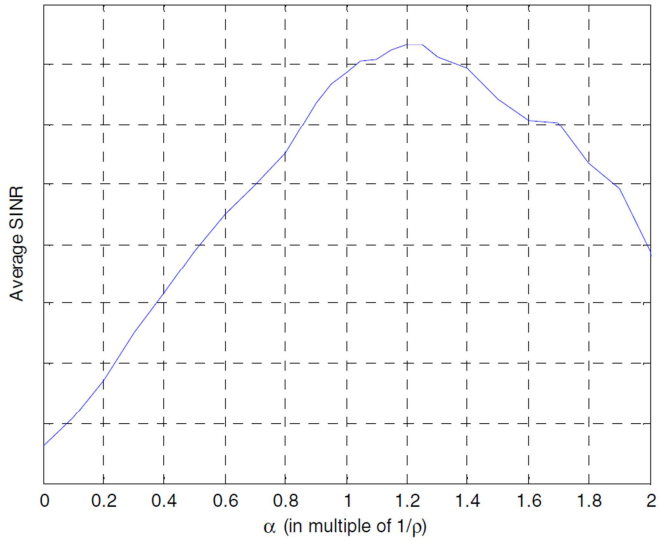

Figure 2.7 Average SINR versus regularized inverse parameter α as a multiple of $1/\rho$, for M = K = 10, ρ = 14 dB. The value α = 0 corresponds to channel inversion. Increasing α at first increases the SINR by reducing γ. However, as α increases further, the interference created by the regularized inverse overcomes the advantage obtained from reducing γ.

2.7.2 Simulation of a complete system

To check the distance from capacity, the authors of the technique simulated a complete system for M = K = 4 antennas/users and M = K = 10 antennas/users. The transmitted signal is

$$\mathbf{x} = \frac{1}{\sqrt{\gamma}} H^*(HH^* + \alpha I)^{-1}(\mathbf{u} + \tau\boldsymbol{\ell}). \tag{2.56}$$

The receivers know τ, but not $\boldsymbol{\ell}$. The K users receive (as a vector)

$$\mathbf{b} = \frac{1}{\sqrt{\gamma}} HH^*(HH^* + \alpha I)^{-1}(\mathbf{u} + \tau\boldsymbol{\ell}) + \mathbf{w}. \tag{2.57}$$

User k models its received signal as

$$y_k = \frac{1}{\sqrt{\gamma}}(u_k + \tau l_k) + w_k' \tag{2.58}$$

where w_k' contains not only the receiver noise w_k, but also the crosstalk from other users introduced by α. Each user then passes this signal through a modulo function that removes the effects of the unknown l_k, and uses a turbo decoder to decode its intended data u_k. Since we are making comparisons with the ergodic sum-capacity (2.5), we allow the channel matrix H to be chosen randomly with every use. This randomly chosen effect is obtained on a smoothly varying channel by

using an interleaver[7] over a long block of many consecutive channel uses. To compare the results with the sum-capacity, we first examine both $M = K = 4$ and $M = K = 10$, using 16-QAM constellations with either rate $r = 1/2$ (2 bitinfo/symbol) and rate $r = 3/4$ (3 bitinfo/symbol) codes. The sum rate is therefore

$$R_{\text{sum}} = 4rK \text{ [bits/channel use]}. \tag{2.59}$$

The possible sum-rates for $r = 1/2$ are, therefore, $R_{\text{sum}} = 8$ [bits/channel use] and for and $R_{\text{sum}} = 20$ for $K = 4$ and $K = 10$, respectively. The sum-rates for $r = 3/4$ are $R_{\text{sum}} = 12$ and $R_{\text{sum}} = 30$. To find the receiver operating points that correspond to these sum rates, we turn to Figure 2.8, which shows the sum capacity for $K = 4$ and $K = 10$ systems as a function of $\rho = 1/\sigma^2$. These sum-capacity curves are computed by evaluating (2.5) numerically (details are omitted). The operating point for $r = 1/2$ is approximately $\rho = 7$ dB for either $K = 4$ or $K = 10$, and the operating point for $r = 3/4$ is approximately $\rho = 11.2$ dB for either K.

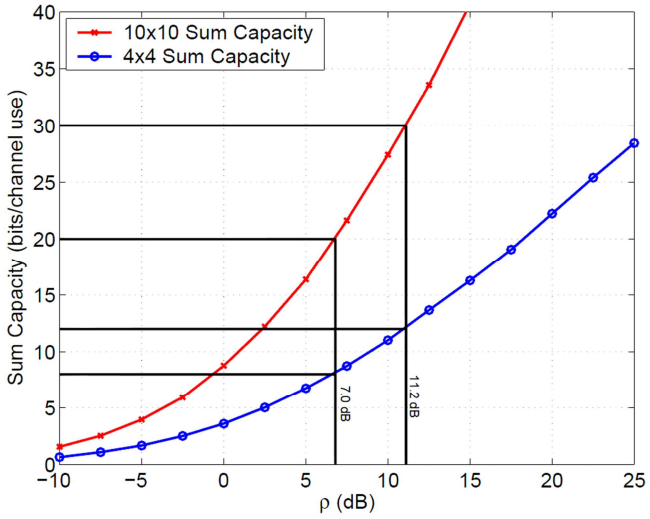

Figure 2.8 Sum-capacity for $M = K = 4$ (blue curve) and $M = K = 10$ (red curve) as a function of the receiver additive-noise variance. The marker lines shows that to achieve $C = 8$ ($K = 4$) or $C = 20$ ($K = 10$), the (reciprocal) noise variance must be $\rho = 1/\sigma^2 = 7$ dB. For $C = 12$ ($K = 4$) or $C = 30$ ($K = 10$), the noise variance must be $\rho = 1/\sigma^2 = 11.2$ dB.

[7] Interleaving is a way to arrange data in a non-contiguous way to increase performance.

2.8 Discussion

Even if we transmit at very high sum-rates (ten of bits/channel use), we are reasonably close to capacity. There are ways to get closer, like transmit at higher rates to the users whose channels happen to be best, since the sum-capacity is not necessarily attained by transmitting at equal rates to all of the users, or compute and overcome the penalty for using the modulo operation at the receiver.

We have almost no analysis of the combination of regularization and perturbation, nor do we have any information-theoretic limit for the basic perturbation method. Although not rigorous, the analysis of γ in Section 2.6.2 predicts the approximate behavior of the integer minimization (2.36), and suggests that the basic perturbation algorithm should work for any K, limited only by the complexity of the minimization (2.36). The sphere encoder allows us to handle up to $K = 15$ with relative ease. The transmitter power-normalization constant γ seems to go to a limiting constant as $K \to \infty$, implying that we may be a fixed distance from the sum-capacity for any K. We would like a theory that predicts the limiting value of γ as $K \to \infty$.

Another area we treated only superficially is computing the exact effect on performance of normalizing at the transmitter with $\sqrt{\gamma}$, versus normalizing with $\sqrt{\mathrm{E}[\gamma]}$ (see 2.3 and 2.4). The most practical choice is $\sqrt{\mathrm{E}[\gamma]}$, because the receivers then do not need to know γ. We, however, chose $\sqrt{\gamma}$ for three reasons:

1) $\mathrm{E}[\gamma]$ does not need to exist;
2) It is simpler in the simulations to instantly compute $\sqrt{\gamma}$ rather than to compute $\mathrm{E}[\gamma]$;
3) It has found the performance difference to be very small. For example, it has shown in Figure 2.9 the bit probability of error for rate $r = 3/4$ turbo-encoded data using 16-QAM symbols when normalizing by $\sqrt{\gamma}$ (instantaneous) and by $\sqrt{\mathrm{E}[\gamma]}$ (average). We see that the performance is actually improved very slightly by normalizing by $\sqrt{\mathrm{E}[\gamma]}$.

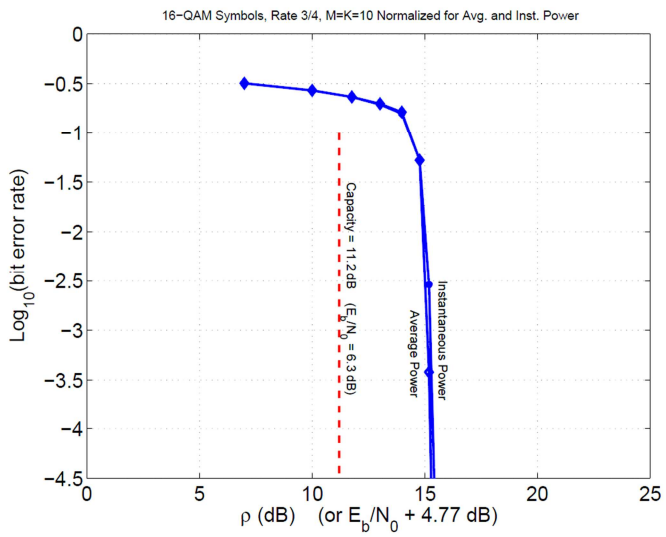

Figure 2.9 Bit probability of error for rate $r = 3/4$ turbo-encoded data using 16-QAM symbols, for $M = K = 10$. The curve on the right (instantaneous power constraint) uses normalization at the transmitter by $\sqrt{\gamma}$; the curve on the left (average power constraint) uses normalization by $\sqrt{\mathrm{E}[\gamma]}$. The difference in performance is small.

When the transmitter normalizes by $\sqrt{\mathrm{E}[\gamma]}$, the receivers do not need to know anything at all about the channel for the techniques to work. Perhaps we should be comparing the results with the channel capacity that is attained when only the transmitter knows the channel. Unfortunately, this capacity is apparently not as easy to compute as when both transmitter and receivers know the channel.

We have not analyzed the optimum τ to choose; for example, increasing τ reduces decoding errors due to the mod-operation, but increases γ. Finally, we have also not discussed how to handle users with differing average received signal power. This extension would be particularly useful for systems where there are many users, and some are much nearer to the access point than others.

Chapter 3

A CONTINUOS VECTOR PERTURBATION [10]

The sum-rate of the broadcast channel in a MIMO communication system can be further improved by using a new technique, which adds a *continuous perturbation* to the data. The perturbation vector will be treated as interference at the receiver, thus it will be transparent to the receiver. The derivation of the continuous vector perturbation is provided by maximizing the SINR or minimizing the minimum mean square error of the received signal.

3.1 Introduction

The model for the forward link is the same of Section 2.2; it includes a base-station with M transmit antennas and K users, each with one received antenna. Previously it has shown that the first approach is to multiply a precoding matrix G ($G = H^*(HH^* + \alpha I)^{-1}$ in the regularized perturbation of Section 2.7) to the data vector $\mathbf{u}$ at the base-station before transmitting. This technique is commonly known as *precoding*. Besides precoding, the base-station can also add perturbation to the data vector $\mathbf{u}$ called *vector perturbation*. It has been shown that by adding a discrete perturbation vector $\tau\boldsymbol{\ell}$, where τ is a constant value and $\boldsymbol{\ell}$ is a vector consisting of only integer value, to the data vector, can reduce the energy of the transmitted signal so as to achieve excellent sum-rate. In this chapter a new perturbation technique that uses a continuous perturbation vector to improve the performance of multi-antenna multi-user communication system is presented. Moreover, when we combine the continuous perturbation with the discrete perturbation, the performance is better than with only the discrete perturbation alone.

3.2 Continuous perturbation

3.2.1 With continuous perturbation only

In this section, we propose a continuous perturbation, where $\tau\boldsymbol{\ell} = \mathbf{p}$. It is different from discreet perturbation, where $\boldsymbol{\ell}$ consists of only integers, $\mathbf{p}$ can be any real or complex value.

When inverse precoding, $G = H^*(HH^*)^{-1}$, is used, the received signal is

$$\mathbf{y} = H\frac{G(\mathbf{u}+\mathbf{p})}{\sqrt{\gamma}} + \mathbf{w} = H\frac{H^*(HH^*)^{-1}(\mathbf{u}+\mathbf{p})}{\sqrt{\gamma}} + \mathbf{w} = \frac{(\mathbf{u}+\mathbf{p})}{\sqrt{\gamma}} + \mathbf{w}. \tag{3.1}$$

Where $\mathbf{u}/\sqrt{\gamma}$ is the desired signal, $\mathbf{p}/\sqrt{\gamma}$ is considered interference to the decoder, and $\mathbf{w}$ is the AWGN.

The main objective of adding a continuous vector $\mathbf{p}$ to the data vector is to achieve a higher throughput. Thus, an obvious choice of $\mathbf{p}$ is to maximize the SINR

$$\text{SINR} = \frac{\|\mathbf{u}\|^2}{\|\mathbf{p}\|^2 + \gamma K\sigma^2}. \tag{3.2}$$

The normalization constant γ is

$$\gamma = \|G(\mathbf{u}+\mathbf{p})\|^2 = \mathbf{u}^*G^*G\mathbf{u} + 2\text{Re}(\mathbf{u}^*G^*G\mathbf{p})\mathbf{p}^*G^*G\mathbf{p}. \tag{3.3}$$

When (3.2) and (3.3) combined, it becomes

$$\text{SINR} = \frac{\mathbf{u}^*\mathbf{u}}{\mathbf{p}^*\mathbf{p} + K\sigma^2(\mathbf{u}^*G^*G\mathbf{u} + 2\text{Re}(\mathbf{u}^*G^*G\mathbf{p}) + \mathbf{p}^*G^*G\mathbf{p})} = \frac{\mathbf{u}^*\mathbf{u}}{D} \tag{3.4}$$

where

$$D = \mathbf{p}^*(I + K\sigma^2G^*G)\mathbf{p} + 2K\sigma^2\text{Re}(\mathbf{u}^*G^*G\mathbf{p}) + K\sigma^2\mathbf{u}^*G^*G\mathbf{u}.$$

Since $\mathbf{p}$ is continuous, unlike the sphere encoding scheme in Section 2.6 which is a discrete value, it can be optimized analytically. Next, we are going to derive $\mathbf{p}$ by maximizing the SINR, in other words, we take the derivative of (3.4), we can maximize SINR by minimizing its denominator D by taking the derivative of D with respect to $\mathbf{p}$.

$$\frac{\partial D}{\partial \mathbf{p}} = 2(I + K\sigma^2G^*G)\mathbf{p} + 2K\sigma^2G^*G\mathbf{u}. \tag{3.5}$$

Next, we let ${\partial D}/{\partial \mathbf{p}} = 0$, to find the optimal $\mathbf{p}$

$$\mathbf{p} = -K\sigma^2(I + K\sigma^2G^*G)^{-1}G^*G\mathbf{u}. \tag{3.6}$$

Similarly, we can maximize the total mean square error (MSE) of the received signal to find $\mathbf{p}$. From (3.1), the estimate signal is

$$\hat{\mathbf{u}} = \mathbf{u} + \mathbf{p} + \sqrt{\gamma}\mathbf{w} \tag{3.7}$$

the total mean square error of the received signal is

$$\text{MSE} = \|\hat{\mathbf{u}} - \mathbf{u}\|^2 = \left\|\mathbf{p} + \sqrt{\gamma}\mathbf{w}\right\|^2. \tag{3.8}$$

Thus we can find $\mathbf{p}$ by minimizing (3.8) by taking its derivative

$$\begin{aligned} \frac{\partial \text{MSE}}{\partial \mathbf{p}} &= 2(I + K\sigma^2G^*G)\mathbf{p} + 2K\sigma^2G^*G\mathbf{u} = 0 \\ \mathbf{p} &= -K\sigma^2(I + K\sigma^2G^*G)^{-1}G^*G\mathbf{u}. \end{aligned} \tag{3.9}$$

It can be seen that (3.9) is the same as (3.6), this implies that $\mathbf{p}$ can be found by using either maximizing the SINR or minimizing the total mean square error of the received signal.

3.2.2 Combine continuous perturbation with discrete perturbation

In this section we are going to investigate the effect of continuous perturbation when it is combined with the discrete perturbation. When both the discrete perturbation $\tau\boldsymbol{\ell}$ and continuous perturbation $\mathbf{p}$ to the data vector $\mathbf{u}$, i.e. $\mathbf{v} = \tau\boldsymbol{\ell} + \mathbf{p}$, the received signal becomes

$$\mathbf{y} = H\frac{G(\mathbf{u} + \tau\boldsymbol{\ell} + \mathbf{p})}{\sqrt{\gamma}} + \mathbf{w} = \frac{(\mathbf{u} + \tau\boldsymbol{\ell} + \mathbf{p})}{\sqrt{\gamma}} + \mathbf{w} = \frac{\mathbf{u}}{\sqrt{\gamma}} + \frac{\tau\boldsymbol{\ell}}{\sqrt{\gamma}} + \frac{\mathbf{p}}{\sqrt{\gamma}} + \mathbf{w}. \tag{3.10}$$

Where $\mathbf{u}/\sqrt{\gamma}$ is the desired signal, $\tau\boldsymbol{\ell}/\sqrt{\gamma}$ will be removed by the modulo function, $\mathbf{p}/\sqrt{\gamma}$ is considered interference to the decoder, and $\mathbf{w}$ is the AWGN.

The normalization constant γ is

$$\gamma = \|G(\mathbf{u} + \tau\boldsymbol{\ell} + \mathbf{p})\|^2$$

The value of τ is known to the receiver, hence the second term on the right hand side of (3.10) can be removed by the modulo function (2.35).

Since the vector perturbation consists of both the continuous and discrete vectors, the cost function of finding $\boldsymbol{\ell}$ by minimizing γ in Section 2.6.1 is no longer valid. It is found contradicting as the value of $\mathbf{p}$ becomes $-\boldsymbol{\ell}$ to satisfy the cost function, thus resulting in canceling the discrete perturbation. Thus, when we find the continuous perturbation, the discrete perturbation can be added to the data vector $\mathbf{u}$ to find $\mathbf{p}$. As a result, the continuous perturbation $\mathbf{p}$ becomes

$$\mathbf{p} = -K\sigma^2(I + K\sigma^2 G^*G)^{-1}G^*G(\mathbf{u} + \tau\boldsymbol{\ell}). \tag{3.11}$$

In this case, the choice of integer vector $\boldsymbol{\ell}$ is found concurrently with the continuous vector $\mathbf{p}$, which is made with the modified cost function that minimizes the total mean square expected received signal.

From (3.10), the estimate signal is

$$\hat{\mathbf{u}} = \mathbf{u} + \mathbf{p} + \sqrt{\gamma}\mathbf{w} \tag{3.12}$$

hence, the total mean square error of the received signal is

$$\text{MSE} = \|\hat{\mathbf{u}} - \mathbf{u}\|^2 = \left\|\mathbf{p} + \sqrt{\gamma}\mathbf{w}\right\|^2. \tag{3.13}$$

The choice of $\boldsymbol{\ell}$ and $\mathbf{p}$ is found by minimizing (3.13)

$$(\mathbf{p}, \boldsymbol{\ell}) = \arg\min_{\mathbf{p}', \boldsymbol{\ell}'} \left\|\mathbf{p}' + \sqrt{\gamma}\mathbf{w}\right\|^2. \tag{3.14}$$

Since $\mathbf{p}$ is given in (3.11), when we combine (3.11) and (3.14), the choice of $\boldsymbol{\ell}$ becomes

$$\begin{aligned}\boldsymbol{\ell} = \arg\min_{\boldsymbol{\ell}'} \Big\| &-K\sigma^2(I + K\sigma^2 G^*G)^{-1}G^*G(\mathbf{u} + \tau\boldsymbol{\ell}') \\ &+ \sqrt{\mathbf{u}^*G^*G\mathbf{u} + \boldsymbol{\ell}'^*G^*G\boldsymbol{\ell}' + \mathbf{p}^*G^*G\mathbf{p} + 2\text{Re}(\mathbf{u}^*G^*G\mathbf{p}) + 2\text{Re}(\mathbf{u}^*G^*G\boldsymbol{\ell}') + 2\text{Re}(\boldsymbol{\ell}'^*G^*G\mathbf{p})}\sqrt{K\sigma^2}\Big\|^2\end{aligned} \tag{3.15}$$

or

$$\boldsymbol{\ell} = \arg\min_{\boldsymbol{\ell}'} \left\|\mathbf{p}' + \sqrt{\gamma}\mathbf{w}\right\|^2 \tag{3.16}$$

where

$$\gamma = \mathbf{u}^*G^*G\mathbf{u} + \boldsymbol{\ell}'^*G^*G\boldsymbol{\ell}' + \mathbf{p}^*G^*G\mathbf{p} + 2\text{Re}(\mathbf{u}^*G^*G\mathbf{p}) + 2\text{Re}(\mathbf{u}^*G^*G\boldsymbol{\ell}') + 2\text{Re}(\boldsymbol{\ell}'^*G^*G\mathbf{p})$$

3.3 Simulations results

Figure 3.1 and Figure 3.2 compare inverse precoding with continuous perturbation to the inversion and regularize inversion precoding without perturbation using uncoded QPSK and 16-QAM with $M = K = 4$ respectively.

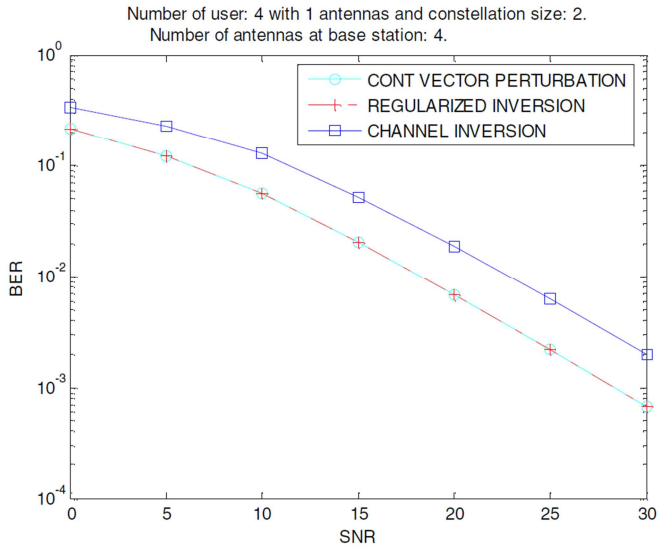

Figure 3.1 Probability of bit error of inverse precoding with continuous perturbation, inverse and regularize-inversion without perturbation using uncoded QPSK symbols, M=K=4.

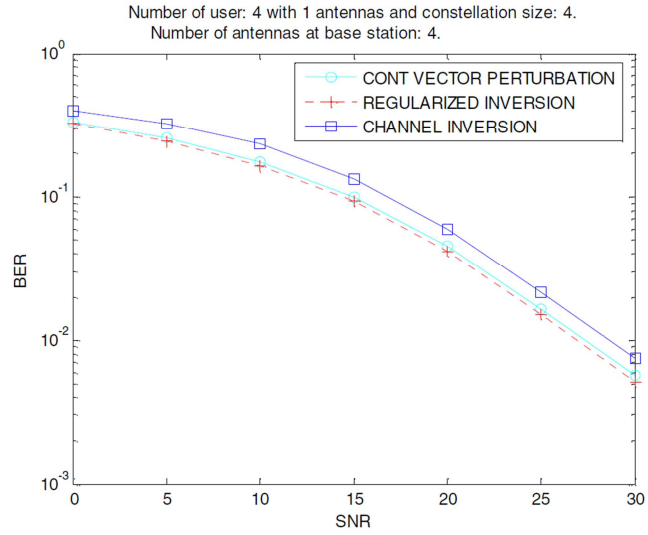

Figure 3.2 Probability of bit error of inverse precoding with continuous perturbation, inverse and regularize-inversion without perturbation using uncoded 16QAM symbols, M=K=4.

In the case of QPSK, the probability of bit error of the inverse precoding with continuous vector perturbation is identical to regularize-inverse precoding without perturbation. Moreover, it has a 5dB gain over the same precoding without perturbation. Likewise, the difference in probability of bit error between the inverse precoding continuous vector perturbation and the regularize-inverse precoding without perturbation is negligible for 16QAM. However the inversion precoding with continuous perturbation is at least 2dB better than the same precoding without continuous perturbation. It is

worth to note that from the results of Figure 3.1 and Figure 3.2, continuous perturbation can be used for any constellation symbols. The comparison of the three techniques using turbo coded 16QAM with $M = K = 4$, using with symbol rate ½ and ¼ respectively is shown in Figure 3.3 and Figure 3.4. The difference between the inverse precoding with continuous vector perturbation and the regularize-inverse precoding without any perturbation at turbo coded rate ½ and ¼ is 0.5dB and 1dB respectively. However, inverse precoding with continuous vector perturbation is 1.5dB and 2.5dB better than the same precoding without perturbation at turbo coded rate ½ and ¼ respectively.

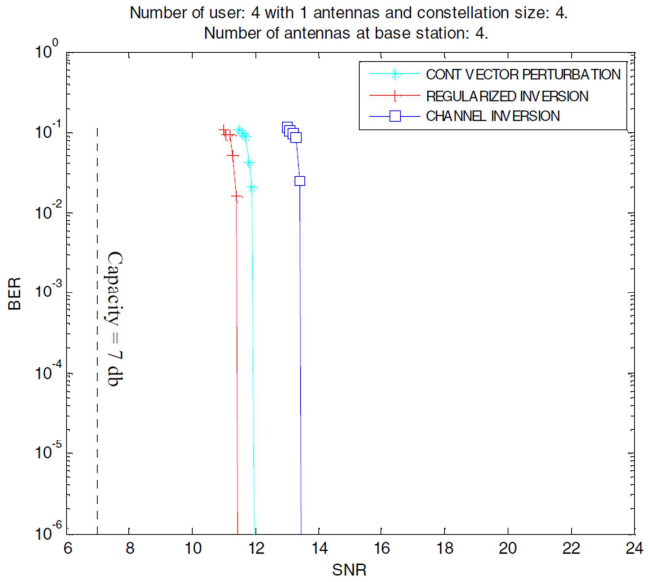

Figure 3.3 Probability of bit error of inverse precoding with continuous perturbation, inverse and regularize-inversion without perturbation using rate ½ turbo coded 16QAM symbols, M=K=4.

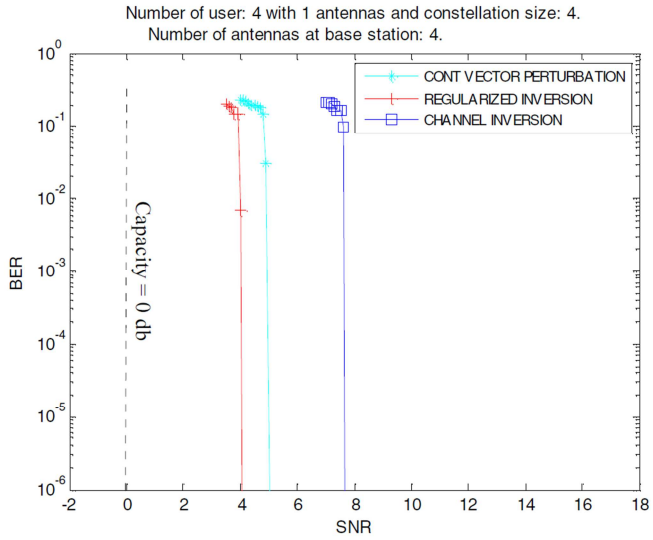

Figure 3.4 Probability of bit error of inverse precoding with continuous perturbation, inverse and regularize-inversion without perturbation using rate ¼ turbo coded 16QAM symbols, M=K=4

The results in Figure 3.5 shows the probability of bit error of inverse precoding with continuous plus discrete perturbation is better than inverse precoding with discrete perturbation and regularize-inverse precoding with discrete perturbation by 1.5dB and 0.5dB respectively.

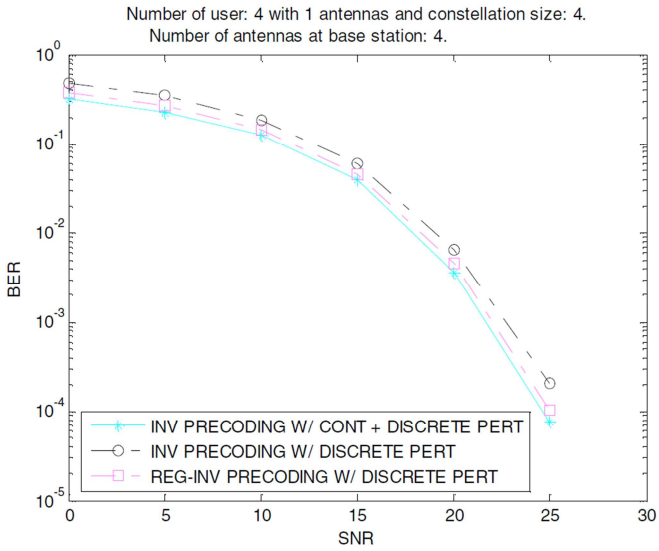

Figure 3.5 Probability of bit error of inverse precoding with continuous plus discrete perturbation, inverse and regularize-inversion with discrete perturbation using uncoded 16QAM symbols, M=K=4.

3.4 Conclusions

In this chapter, we show that by adding a continuous vector perturbation to the data vector, which is treated as interference by the receiver, can achieve a better decoding performance than the system without perturbation.

It is also worth to note that when the continuous perturbation is combined with discrete perturbation, the performance of the inverse precoding continuous plus discrete perturbation is better than inverse precoding or regularize inverse precoding with discrete perturbation only.

REFERENCES

[1] M. Costa, "Writing on dirty paper," *IEEE Trans. Information Theory*, vol. 29, pp. 439–441, May 1983.

[2] C. B. Peel, B. M. Hochwald, and A. L. Swindlehurst, "A vector-perturbation technique for near-capacity multiantenna multiuser communication— Part I: Channel inversion and regularization," *IEEE Trans. Commun.*, vol. 53, pp. 195–202, Jan. 2005.

[3] C. B. Peel, B. M. Hochwald, and A. L. Swindlehurst, "A Vector-Perturbation Technique for Near-Capacity Multi-Antenna Multi-User Communication—Part II: Perturbation," *IEEE Trans. Commun.*, vol. 53, pp. 573–544, Mar. 2005.

[4] M. Tomlinson, "New automatic equaliser employing modulo arithmetic," *Electron. Lett.*, vol. 7, pp. 138–139, Mar. 1971.

[5] H. Harashima and H. Miyakawa, "Matched-transmission technique for channels with intersymbol interference," *IEEE Trans. Commun.*, vol. COM-20, pp. 774–780, Aug. 1972.

[6] U. Fincke and M. Pohst, "Improved methods for calculating vectors of short lengths in a lattice, including a complexity analysis," *Math. Computat.*, vol. 44, pp. 463–471, Apr. 1985.

[7] E. Agrell, T. Eriksson, A. Vardy, and K. Zeger, "Closest point searches in lattices," *IEEE Trans. Inf. Theory*, vol. 48, pp. 2201–2214, Aug. 2002.

[8] M. O. Damen, A. Chkeif, and J.-C. Belfiore, "Lattice code decoder for space–time codes," *IEEE Commun. Lett.*, vol. 4, pp. 161–163, May 2000.

[9] B. Daneshrad, "MIMO: The next revolution in wireless data communications", *RF Design Magazine,* Apr. 2008.

[10] W. S. Chua, C. Yuen and F. Chin, "A continuous vector-perturbation for multi-antenna multi-user communication," in *Proceeding of VTC2007-Spring*, (Dublin, Ireland), pp. 1806-1810, Apr. 22-25, 2007.

[11] C. Windpassinger, R. F. H. Fischer, and J. B. Huber, "Lattice-reduction-aided broadcast precoding," *IEEE Trans. Comm.*, vol. 52, pp. 2057-2060, Dec. 2004.

[12] C. Yuen and B. M. Hochwald, "How to gain 1.5 dB in vector precoding," in *Proceedings of Globecom 2006,* (San Francisco, USA), p. 5 pages, Nov. 27 – Dec. 1, 2006.